

## The relationship between local order, long range order, and sub-band-gap defects in hafnium oxide and hafnium silicate films

D. H. Hill,<sup>1</sup> R. A. Bartynski,<sup>1,a)</sup> N. V. Nguyen,<sup>2</sup> Albert G. Davydov,<sup>2</sup> Deane Chandler-Horowitz,<sup>2</sup> and Martin M. Frank<sup>3</sup>

<sup>1</sup>*Department of Physics and Astronomy and Laboratory for Surface Modification, Rutgers University, Piscataway, New Jersey 08854, USA*

<sup>2</sup>*National Institute of Standards and Technology, Gaithersburg, Maryland 20899, USA*

<sup>3</sup>*IBM Thomas J. Watson Research Center, Yorktown Heights, New York 10598, USA*

(Received 16 November 2007; accepted 6 March 2008; published online 9 May 2008)

We have measured x-ray absorption spectra (XAS) at the oxygen *K* edge for hafnium oxide (HfO<sub>2</sub>) films grown by chemical vapor deposition (CVD) and atomic layer deposition (ALD), as well as for hafnium silicate (HfSiO) films grown by CVD. The XAS results are compared to x-ray diffraction (XRD) and spectroscopic ellipsometry (SE) data from the same films. Features characteristic of crystalline HfO<sub>2</sub> are observed in the XAS spectra from all CVD-grown HfO<sub>2</sub> films, even for a thickness of 5 nm where XRD is not sensitive. XAS and XRD spectra from the ALD-grown HfO<sub>2</sub> films exhibit the signature of crystallinity only for films that are 20 nm or thicker. These characteristic XAS features are absent in all HfSiO films measured, which is consistent with their being amorphous. The appearance of these peaks in XAS and XRD is correlated with sub-band-gap absorption in the SE spectra, which appears to be intrinsic to crystalline HfO<sub>2</sub> in the monoclinic phase. © 2008 American Institute of Physics. [DOI: 10.1063/1.2909442]

The historic increase in semiconductor logic integration relies on exponential downscaling in the size of individual metal-oxide-semiconductor field-effect transistors. As the capacitance of the gate insulator stack needs to be increased simultaneously with a reduction in channel length to maintain gate control over the inversion layer, this has led to a reduction in SiO<sub>2</sub> or SiON gate insulator thickness to ~1 nm in high-performance logic chips. Despite the nearly perfect electrical properties of the SiO<sub>2</sub>/Si interface, at sub-nanometer thicknesses, electron tunneling through the oxide results in an unacceptably high gate leakage current even at modest biases. This has led to a large body of research aimed at replacing SiO<sub>2</sub> with a high-permittivity (high-*K*) dielectric which could provide the needed capacitance for a thicker film, thus mitigating the leakage current problem.<sup>1-4</sup> Hafnium oxide (HfO<sub>2</sub>) and hafnium silicates (HfSiO) are promising candidate high-*K* dielectrics. However, questions remain regarding the impact of structural properties such as crystallinity on electrical performance. Crystallinity of Hf-based dielectrics depends on factors such as composition, thickness, deposition conditions, and thermal budget during device integration which usually involves annealing at 1000 °C or more. A number of reasons, often speculative, have been put forward for aiming to keep high-*K* dielectrics amorphous: (a) heterogeneous grain orientations could give rise to spatially varying electric fields in the channel, causing carrier scattering and degrading mobility. (b) Grains could cause device-to-device variations in, e.g., leakage or threshold voltage. (c) Grains could increase effective line edge roughness after gate etch. (d) Grain boundaries have been claimed to be responsible for localized unoccupied gap

states,<sup>5-7</sup> e.g., those observed ~0.2–0.3 eV below the conduction band edge if and only if HfO<sub>2</sub> is crystalline;<sup>8</sup> such gap states may explain undesirable electron trapping and gate leakage with HfO<sub>2</sub>.<sup>9,10</sup>

In this work, we report soft x-ray absorption spectroscopy (XAS) measurements performed on a series of HfO<sub>2</sub> and HfSiO films grown by metal organic chemical vapor deposition (MOCVD) and HfO<sub>2</sub> films grown by atomic layer deposition (ALD) to probe the local bonding and short-range order in these systems. Characteristic features associated with crystalline HfO<sub>2</sub> are observed in the XAS spectra from films that also exhibit well-defined peaks, associated with the monoclinic phase, in XRD. These XAS features are even observed for 5 nm thick CVD films where crystallites are too small to be detected by XRD. By comparing the XAS and XRD results with the optical absorption data, we find that the HfO<sub>2</sub> crystalline state and a sub-band-gap optical absorption feature associated with electronic defects, coincide in all cases. Our results suggest that the so-called defect feature need not be attributed to structural distortions of nanocrystalline (~1 nm) particles or to structural modifications at grain boundaries in the films, as has been proposed.<sup>5-7</sup> Rather, these features appear to be intrinsic to the formation of monoclinic HfO<sub>2</sub> crystallites in the films. Our work thus contributes to a fundamental understanding of the electronic structure of HfO<sub>2</sub> and its electrical properties as a candidate gate dielectric.

Measurements were performed on three sets of films. These sets were composed of MOCVD-grown HfO<sub>2</sub> and HfSiO [Hf:Si ~ 80:20] samples, as well as a set of ALD-grown HfO<sub>2</sub> films. Each set contained films of 5, 10, 20, and 40 nm of nominal thicknesses. The MOCVD HfO<sub>2</sub> films were grown using hafnium tetra-*tert*-butoxide [HTB, Hf(OC(CH<sub>3</sub>)<sub>3</sub>)<sub>4</sub>] and O<sub>2</sub>. To grow the HfSiO films, SiH<sub>4</sub> was

<sup>a)</sup>Electronic mail: bart@physics.rutgers.edu.

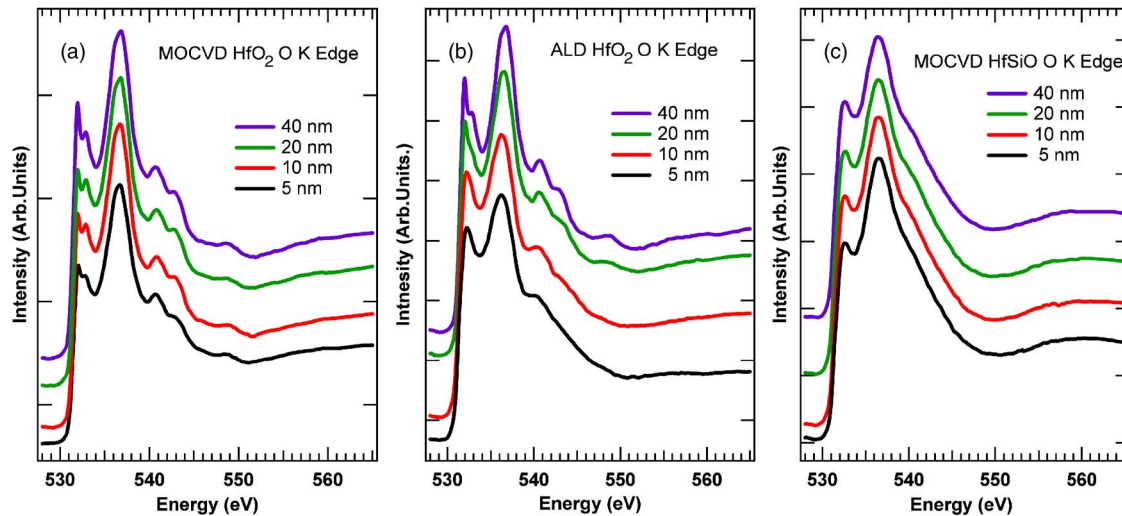


FIG. 1. (Color online) X-ray absorption spectroscopy (XAS) data of the O *K*-edge from HfO<sub>2</sub> films deposited by (a) MOCVD and (b) ALD, as well as (c) MOCVD-grown HfSiO films, for thicknesses of 5, 10, 20, and 40 nm.

added to the precursor mix. The ALD films were deposited via alternating exposures of HfCl<sub>4</sub> and H<sub>2</sub>O using N<sub>2</sub> as a carrier gas. The films were deposited on highly doped 200 mm Si(100) wafers (*n* type, ~1 Ω cm, 800 μm thick) whose surfaces were cleaned by an SC-1/SC-2/HF process followed by thermal oxidation using NO which resulted in the formation of an 11 Å oxynitride interface layer prior to deposition of the high-*K* films.

X-ray absorption spectroscopy (XAS) measurements were performed on the U4A beamline of the National Synchrotron Light Source at Brookhaven National Laboratory. To acquire the O *K*-edge spectra, the photon energy was scanned from 500 to 600 eV in 0.1 eV increments while the total electron yield was measured by monitoring the total photocurrent emitted from the sample. The total energy resolution was 0.1 eV and all data were normalized to the incident flux. X-ray diffraction (XRD) spectra were obtained from a Bruker-AXS D8 general area detector diffraction system with Cu *K*α radiation. Two dimensional 2θ-χ patterns were collected in the 2θ range from 15° to 48° and integrated in χ to obtain the patterns. The spectroscopic ellipsometry measurements were performed on a vacuum ultraviolet spectroscopic ellipsometer. The dielectric functions  $\epsilon = \epsilon_1 + i\epsilon_2$ , where  $\epsilon_1$  and  $\epsilon_2$  are the real and imaginary parts of  $\epsilon$ , respectively, were determined from the analysis of the ellipsometric data.

Figures 1(a)–1(c) show a series of XAS spectra for the O *K*-edge obtained from MOCVD-grown HfO<sub>2</sub>, ALD-grown HfO<sub>2</sub>, and MOCVD-grown HfSiO films, respectively, with thicknesses of 5, 10, 20, and 40 nm. All of the spectra show a similar overall shape composed of two main features, one at ~532.3 eV and the other at ~536.5 eV, followed by a gradually decreasing intensity to ~550 eV, above which the intensity is almost constant. These two main peaks are associated with transitions to unoccupied O 2*p* levels that are hybridized with Hf 5*d* orbitals. The lower energy peak (~532.3 eV) and the higher energy peak (~536.5 eV) are the crystal-field-split *e<sub>g</sub>* and *t<sub>2g</sub>* components, respectively, of the Hf 5*d* manifold.<sup>11,12</sup> Upon closer inspection, however, it

is clear that for all film thicknesses, the spectra from MOCVD-grown HfO<sub>2</sub> films exhibit a significant amount of fine structure that is absent in the spectra from the HfSiO films. In particular, the spectra from the MOCVD-grown HfO<sub>2</sub> films have a series of three well-defined peaks at 540, 542, and 548.5 eV. Emission in this energy range is associated with excitation to O 2*p* levels hybridized with Hf 4*s* and 4*p* states and it is well established that the appearance of these three peaks is a signature of crystalline HfO<sub>2</sub>.<sup>13–18</sup> Another important observation is that the *e<sub>g</sub>*-related feature of the MOCVD-grown HfO<sub>2</sub> films is split into two components at 532.0 and 532.9 eV. In the spectra from the HfSiO films, the absence of this splitting, as well as the lack of the three peaks at higher energies, is consistent with the HfSiO being amorphous for all thicknesses examined here.

In contrast to the MOCVD-grown films of either composition, the XAS spectra from the ALD-grown HfO<sub>2</sub> films change as a function of film thickness. The spectra from the 5 and 10 nm films strongly resemble those from the HfSiO films. The shoulder at 540 eV shows slightly more definition, but the characteristic three peak pattern is absent. On the other hand, the spectra for the 20 and 40 nm films do exhibit the three higher energy peaks, essentially identical to what is observed in the spectra from the MOCVD-grown HfO<sub>2</sub> films. The similarity of these spectra is even more compelling in Fig. 2 where spectra from the 5 and 40 nm films of each type are presented on the same plot. While the relative intensity of the fine structure may slightly vary with film thickness, possibly owing to changing surface-to-volume ratio of the crystallites or (in the ALD case) the presence of a second minor phase, the energies of each feature in the thicker ALD-grown films and the MOCVD-grown HfO<sub>2</sub> films are identical indicating that the ALD-grown films are crystalline for thicknesses ≥20 nm.

To investigate the relationship between local bonding, as probed by XAS, and long range order as probed by x-ray diffraction, we obtained XRD data from the MOCVD-grown and ALD-grown HfO<sub>2</sub> films, which are presented in Figs. 3(a) and 3(b), respectively. Each plot contains data from

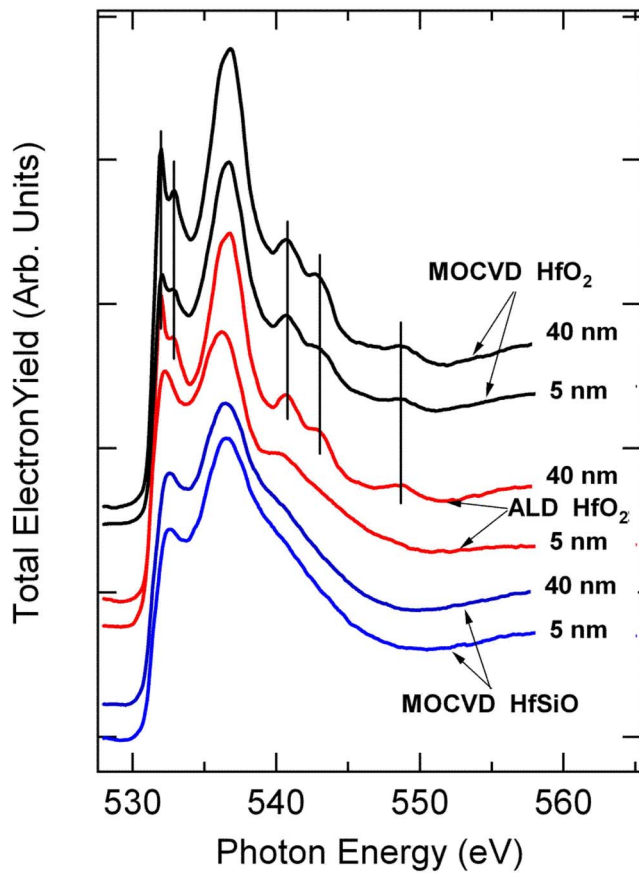


FIG. 2. (Color online) Comparison of selected XAS spectra from Fig. 1.

films with nominal thicknesses of 5, 10, 20, and 40 nm. As evident from Fig. 3(a), well-defined diffraction peaks are present in the data from the 10, 20, and 40 nm MOCVD-grown films. No definitive diffraction features are observed in the 5 nm data due to limited XRD sensitivity. Indexing the peaks for the thicker films shows that the crystallites are in the monoclinic phase. For the ALD-grown films, Fig. 3(b) shows no diffraction features for the 5 and 10 nm thicknesses. The data from the 20 nm film show weak diffraction features while the 40 nm film exhibits well-defined diffraction peaks. Indexing these XRD data shows that most of the peaks are associated with the monoclinic phase, although several weak features suggest the presence of small amounts of material in the orthorhombic or tetragonal phases as well. XRD data obtained from the four HfSiO films [Fig. 3(c)] contain no evidence of diffraction features, indicating that under these deposition and processing conditions, this material remains amorphous up to thicknesses of 40 nm or more.

Figures 4(a)–4(c) summarize the ellipsometric data from CVD-grown HfO<sub>2</sub>, ALD-grown HfO<sub>2</sub>, and CVD-grown HfSiO films, respectively. For all of the HfSiO films, there is an onset at  $\sim 5.75$  eV corresponding to absorption across the band gap of the silicate. In contrast, the data from the CVD-grown HfO<sub>2</sub> films show a pronounced feature at lower energies, with an edge at 5.5 eV that plateaus, followed by a rapid rise above 6 eV. The rapid rise is associated with absorption across the band gap of HfO<sub>2</sub>, while the former feature is attributed to defects  $\sim 0.2$ – $0.3$  eV below the optical band gap.<sup>8</sup> These defects may be the cause of electron trap

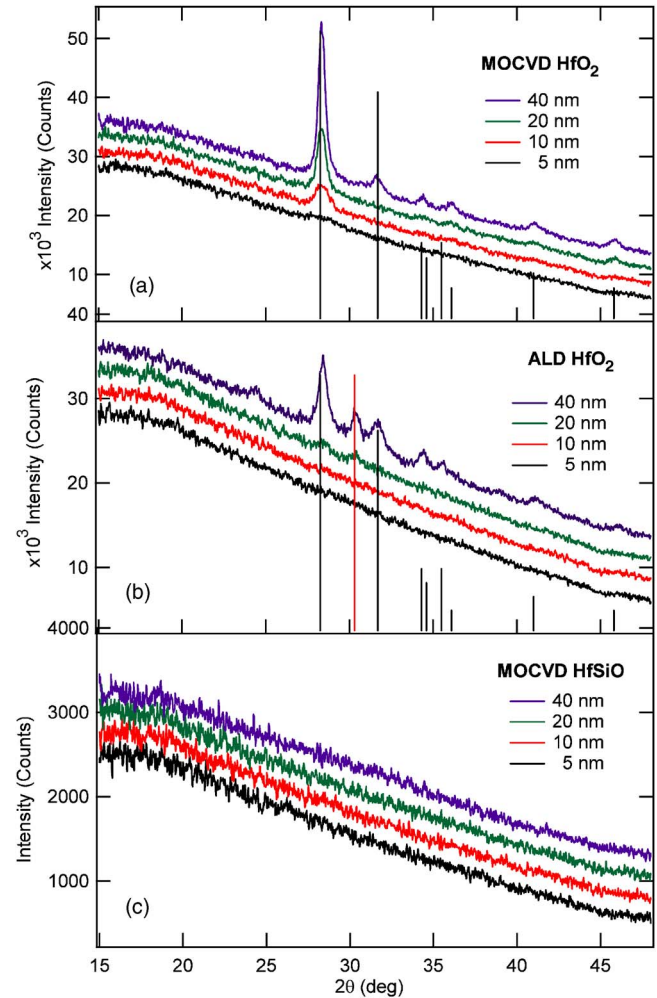


FIG. 3. (Color online) X-ray diffraction (XRD) data from HfO<sub>2</sub> films deposited by (a) MOCVD and (b) ALD, as well as (c) MOCVD-grown HfSiO films. Extra red line in (b) is associated with either orthorhombic or tetragonal phase.

sites in device gate stacks observed at 0.25 and 0.35 eV below the HfO<sub>2</sub> conduction band edge.<sup>10</sup> Although the shape of the HfO<sub>2</sub> absorption edge differs from that of HfSiO, for each material, the shape of the spectrum is the same for all film thicknesses. Figure 4(b) illustrates that this is not the case for the ALD-grown films. For the 5 and 10 nm films, the absorption edge is similar in shape to that of the HfSiO films (i.e., a single onset attributable to transitions across the band gap). In contrast, for the 20 nm film, additional absorption is seen below the energy of the band gap and the 40 nm film has a well-defined sub-band-gap feature that is essentially identical to that seen for the CVD-grown films.

By comparing the XAS data to the XRD and SE data, it is clear that in all cases, films that exhibit XRD peaks associated with monoclinic HfO<sub>2</sub> also show the characteristic three-peaked structure as well as the split peaks at 532.0 and 532.9 eV in XAS and a well-defined sub-band-gap absorption feature in SE. This correlation provides important new information about these material systems. It is well known that XAS spectra are highly sensitive to the local bonding environment of the species whose absorption edge is measured.<sup>11,12</sup> This is primarily because of the participation

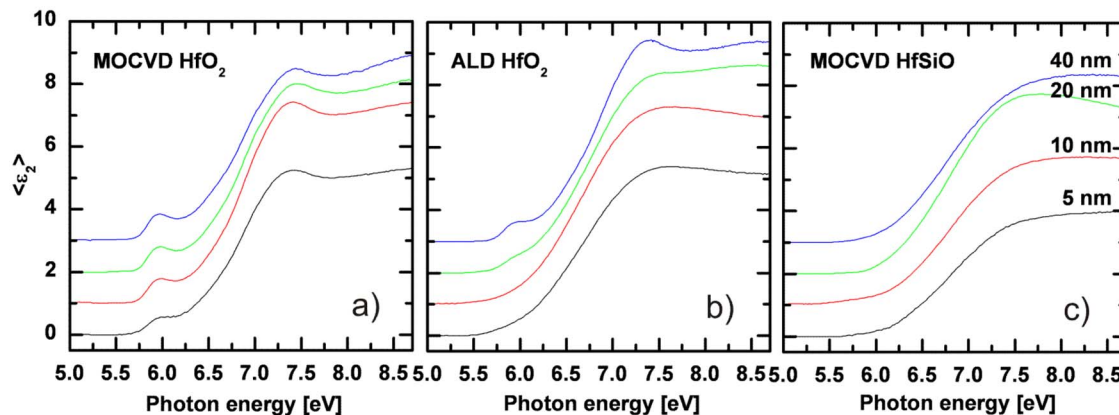


FIG. 4. (Color online) Spectroscopic ellipsometry (SE) data from HfO<sub>2</sub> films deposited by (a) MOCVD and (b) ALD, as well as (c) MOCVD-grown HfSiO films. For clarity, the 10, 20, and 40 nm curves are shifted upward by 1, 2, and 3 units, respectively.

in the absorption process of a core electron whose wave function is highly localized in the atomic site. The XAS data, therefore, reveal the presence of monoclinic HfO<sub>2</sub> nanocrystallites in the 20 nm ALD-grown HfO<sub>2</sub> films and the 5 nm MOCVD-grown films, which are undetected by the less sensitive XRD method. Moreover, there is a one-to-one correlation between the appearance of the monoclinic HfO<sub>2</sub> features in XAS and the presence of the “defect” feature in the optical data. The line shape of the XAS data for the 20 nm ALD film cannot be reproduced by a linear combination of the line shapes for the 40 nm ALD film plus either the 10 or 5 nm ALD film. This speaks against the interpretation that the 20 nm ALD HfO<sub>2</sub> film is composed of a collection of HfO<sub>2</sub> nanocrystallites embedded in an amorphous HfO<sub>2</sub> matrix. Rather, it suggests that the film is dominated by small crystalline nuclei that have not yet been organized to establish long range order.

The splitting of the XAS features associated with the Hf  $e_g$  states (that is, the peaks at 532.0 and 532.9 eV) and the sub-band-gap SE absorption feature have attracted considerable attention in the literature. Recent studies have attributed both phenomena to a Jahn–Teller distortion of the octahedral oxygen cages surrounding Hf ions in nanocrystallites of HfO<sub>2</sub> or at grain boundaries.<sup>5–7</sup> However, the thickness evolution in the data from our films suggests that both phenomena may instead be intrinsic to monoclinic HfO<sub>2</sub>: for MOCVD-grown films, the XAS peak splitting is progressively more well defined as the film thickness increases, indicating increasing crystallite size and therefore a decreasing density of grain boundaries; however, the fraction of the SE absorption intensity attributed to the sub-band-gap feature remains almost constant. The discrepancy between these thickness trends appears to be inconsistent with an assignment to grain boundaries. This observation is similar to what was found in recent optical absorption experiments from sputter-deposited HfO<sub>2</sub> films where increasing intensity of the sub-band-gap feature is correlated with increasing monoclinic crystallinity of the film.<sup>19</sup> One could imagine that the sub-band-gap feature observed in our SE data could be due to O vacancies. However, the films studied here were deposited under oxidizing conditions and both the SE feature and the  $\sim 0.9$  eV splitting in the XAS data are observed. More-

over, in a SE study of HfO<sub>2</sub> films deposited by ALD and annealed in N<sub>2</sub>,<sup>20</sup> i.e., under reducing conditions that may be expected to increase the O vacancy concentration, no increase in sub-band-gap absorption intensity was reported. Cluster calculations modeling the XAS spectrum from O-deficient HfO<sub>2</sub> suggest that the near-edge splitting may be reduced rather than enhanced, for Hf ions near the O vacancy.<sup>21</sup> Both of these observations make O vacancies an unlikely explanation for the sub-band-gap feature or the splitting in the XAS.

Therefore, we propose that the sub-band-gap feature and the splitting in XAS may be intrinsic properties of monoclinic HfO<sub>2</sub>. Indeed, a recent cluster calculation of HfO<sub>2</sub> in the monoclinic structure shows that the near-edge region is dominated by the <sup>2</sup>S and <sup>2</sup>P configurations which form two well-defined features separated by  $\sim 1.25$  eV, very similar to the 0.9 eV splitting we observe,<sup>21</sup> and further supporting our proposal.

In summary, we have obtained O  $K$ -edge XAS spectra from 5, 10, 20, and 40 nm films of HfO<sub>2</sub> and HfSiO grown by CVD and HfO<sub>2</sub> films grown by ALD, and correlated the results with XRD and SE data from the same samples. All of the CVD-grown, as well as the two thickest ALD-grown, HfO<sub>2</sub> films are crystalline and show well-defined features in XAS that are absent from the amorphous samples. The XAS data indicate that monoclinic HfO<sub>2</sub> nanocrystallites are present in the 5 nm CVD-grown and the 20 nm ALD-grown HfO<sub>2</sub> films, even though XRD measurements are inconclusive. A splitting in the XAS spectra near threshold is correlated with sub-band-gap absorption in the SE spectra in all cases. The persistence of these features with increasing film thickness and improved crystallinity suggest that they are intrinsic to crystalline HfO<sub>2</sub> in the monoclinic phase.

R. A. B. and D. H. H. gratefully acknowledge support from the SRC. Use of the National Synchrotron Light Source, Brookhaven National Laboratory, was supported by the U. S. Department of Energy, Office of Science, Office of Basic Energy Sciences, under Contract No. DE-AC02-98CH10886.

- <sup>1</sup>E. P. Gusev, V. Narayanan, and M. M. Frank, *IBM J. Res. Dev.* **50**, 387 (2006).
- <sup>2</sup>*Materials Fundamentals of Gate Dielectrics*, edited by A. A. Demkov and A. Navrotsky (Springer, Dordrecht, 2005).
- <sup>3</sup>J. Robertson, *Rep. Prog. Phys.* **69**, 327 (2006).
- <sup>4</sup>G. D. Wilk, R. M. Wallace, and J. M. Anthony, *J. Appl. Phys.* **89**, 5243 (2001).
- <sup>5</sup>G. Lucovsky, *Appl. Surf. Sci.* **253**, 311 (2006).
- <sup>6</sup>G. Lucovsky, C. C. Fulton, Y. Zhang, Y. Zou, J. Luning, L. F. Edge, J. L. Whitten, R. J. Nemanich, H. Ade, D. G. Schlom, V. V. Afanase'v, A. Stesmans, S. Zollner, D. Triyoso, and B. R. Rogers, *IEEE Trans. Device Mater. Reliab.* **5**, 65 (2005).
- <sup>7</sup>G. Lucovsky, Y. Zhang, J. Luning, V. V. Afanase'v, A. Stesmans, S. Zollner, D. Triyoso, B. R. Rogers, and J. L. Whitten, *Microelectron. Eng.* **80**, 110 (2005).
- <sup>8</sup>N. V. Nguyen, A. V. Davydov, D. Chandler-Horowitz, and M. M. Frank, *Appl. Phys. Lett.* **87**, 192903 (2005).
- <sup>9</sup>X. Xu, M. Houssa, S. De Gendt, and M. Heyns, *Appl. Phys. Lett.* **80**, 1975 (2002).
- <sup>10</sup>G. Bersuker, J. H. Sim, C. S. Park, C. D. Young, S. Nadkarni, R. Choi, and B. H. Lee, *IEEE 44th Annual International Reliability Physics Symposium Proceedings*, 179 (2006).
- <sup>11</sup>F. M. F. de Groot, M. Grioni, J. C. Fuggle, J. Ghijsen, G. A. Sawatzky, and H. Petersen, *Phys. Rev. B* **40**, 5715 (1989).
- <sup>12</sup>L. Soriano, M. Abbate, J. C. Fuggle, M. A. Jimenez, J. M. Sanz, C. Mythen, and H. A. Padmore, *Solid State Commun.* **87**, 699 (1993).
- <sup>13</sup>M. H. Cho, K. B. Chung, C. N. Whang, D. W. Lee, and D. H. Ko, *Appl. Phys. Lett.* **87**, 242906 (2005).
- <sup>14</sup>M. H. Cho, D. W. Moon, S. A. Park, Y. K. Kim, K. Jeong, S. K. Kang, D. H. Ko, S. J. Doh, J. H. Lee, and N. I. Lee, *Appl. Phys. Lett.* **84**, 5243 (2004).
- <sup>15</sup>H. Takahashi, J. Okabayashi, S. Toyoda, H. Kumigashira, M. Oshima, K. Ikeda, G. L. Liu, Z. Liu, and K. Usuda, *Appl. Phys. Lett.* **89**, 012102 (2006).
- <sup>16</sup>H. Takahashi, J. Okabayashi, S. Toyoda, H. Kumigashira, M. Oshima, K. Ikeda, G. L. Liu, Z. Liu, and K. Usuda, *J. Appl. Phys.* **99**, 113710 (2006).
- <sup>17</sup>H. Takahashi, S. Toyoda, J. Okabayashi, H. Kumigashira, M. Oshima, Y. Sugita, G. L. Liu, Z. Liu, and K. Usuda, *Appl. Phys. Lett.* **87**, 012903 (2005).
- <sup>18</sup>S. Toyoda, J. Okabayashi, H. Kumigashira, M. Oshima, K. Yamashita, M. Niwa, K. Usuda, and G. L. Liu, *J. Appl. Phys.* **97**, 104507 (2005).
- <sup>19</sup>E. E. Hoppe, R. S. Sorbello, and C. R. Aita, *J. Appl. Phys.* **101**, 123534 (2007).
- <sup>20</sup>D. Triyoso, R. Liu, D. Roan, M. Ramon, N. V. Edwards, R. Gregory, D. Werho, J. Kulik, G. Tam, E. Irwin, X.-D. Wang, L. B. La, C. Hobbs, R. Garcia, J. Baker, B. E. White, Jr., and P. Tobin, *J. Electrochem. Soc.* **151**, F220 (2004).
- <sup>21</sup>D.-Y. Cho, J.-M. Lee, S.-J. Oh, H. Jang, J.-Y. Kim, J.-H. Park, and A. Tanaka, *Phys. Rev. B* **76**, 165411 (2007).